Chapter 7
NASA Armstrong's Thermal Vibration Test System (TVTS) Pathfinder Capability

Jessica J. De la Cruz, Keerti K. Bhamidipati, Chris B. Kostyk, Jackson T. Winter, Natalie D. Spivey, Phillip C. Nguyen, and Samson S. Truong

Abstract The National Aeronautics and Space Administration Armstrong Flight Research Center Flight Loads Laboratory is developing a new capability for combined vibration and thermal load testing called the Thermal Vibration Test System. A pathfinder capability has been demonstrated and consisted of a radiant quartz lamp heater installed above a 500-lbf electrodynamic shaker. This passively cooled test fixture was designed to test up to five accelerometers simultaneously at temperatures up to 1000 °F, for durations of up to 75 min. The fixture was used to evaluate accelerometer performance up to 3 grms over a 5 – 300 Hz frequency range for multiple sensors subjected to single-sided heating at temperatures between room temperature and 1000 °F. The shaker was controlled using the Sandia National Laboratory (Albuquerque, New Mexico) "Rattlesnake" vibration controller, programed to trigger vibration test profiles during constant temperature holds. Vibration test data was acquired using the Hottinger Brüel & Kjær LAN-XI data acquisition hardware and BK Connect® software. Separate thermal data acquisition and control systems were used for single thermocouple thermal control and to gather test data from thermocouples installed on the accelerometers and fixture. This combined load test served as a pathfinder to investigate high-temperature sensor measurements and develop larger scale Thermal Vibration Test System capability.

Keywords Testing · Environmental · Durability · Thermal · Vibration

Introduction

The National Aeronautics and Space Administration (NASA) Armstrong Flight Research Center (AFRC) (Edwards, California) has completed a series of test runs to develop a new thermal vibration-combined load testing capability in the Flight Loads Laboratory (FLL). This pathfinder Thermal Vibration Test System (TVTS) served as a platform to work through known challenges of thermal vibration testing (such as accelerometer piezoelectric resistance loss at higher temperatures [1], protecting shaker equipment from heat, and simultaneous thermal and dynamic control of a multi-environment test setup [2]-[6] at a smaller scale and less severe thermal environment than an envisioned full operating capability. In the future, the FLL plans to mature this TVTS capability to larger scale environmental qualification testing for high-temperature sensors.

The pathfinder test setup consisted of a test fixture assembly with a two-story stainless-steel heatsink bolted to a magnesium fixture atop a 500-lbf shaker. The setup was designed to generate a combined thermal-vibration environment on the top of the heat-sink. A quartz lamp radiative heater was installed above this region, and reflective alumina "fences" served both to direct heat to the region and prevent heat spillover to low-temperature hardware. Independent vibration and thermal data acquisition systems were run simultaneously and time synchronized. A central control thermocouple provided feedback to drive closed-loop control, and various additional thermocouple sensors were placed on the top surface of the heatsink to measure the thermal loads. A low-temperature control accelerometer was placed on top of the shaker armature to provide closed-loop control to the vibration fixture. During pathfinder testing, the performance of commercially available accelerometers in a combined thermal-mechanical environment was evaluated. A maximum target test temperature limit of

Jessica J. De la Cruz · Keerti K. Bhamidipati · Chris B. Kostyk · Jackson T. Winter · Natalie D. Spivey · Phillip C. Nguyen · Samson S. Truong
National Aeronautics and Space Administration, Armstrong Flight Research Center, 4800 Lilly Ave, Edwards, CA 93523, USA
e-mail: jessica.j.delacruz@nasa.gov; keerti.k.bhamidipati@nasa.gov; chris.b.kostyk@nasa.gov; jackson.t.winter@nasa.gov; natalie.d.spivey@nasa.gov; phillip.c.nguyen@nasa.gov; samson.s.truong@nasa.gov

Kristin B. Zimmerman, PhD (eds.), *Dynamic Evironments and Durability Testing, 2026, Vol. 7*, Conference Proceedings of the Society for Experimental Mechanics Series, https://doi.org/10.1007/978-8-743-81446-7_7

1000 °F was selected based on the temperature ratings of candidate accelerometers available within the testing time-window. A target shaker level of 3 grms was also identified based on the capabilities of the FLL 500-lbf shaker and weight of the passively cooled test fixture. Five accelerometers and three signal conditioning hardware configurations that were considered promising candidates were evaluated to measure noise in accelerometer signals at elevated temperature, and the ability of the signal conditioning hardware to mitigate that noise. The data obtained from multiple test cases was used to validate the application of the combined loads and the performance of each accelerometer with signal conditioning hardware.

Test Objectives

The purpose of this new pathfinder TVTS capability was to apply combined thermal and vibrational loads and to measure accelerometer characterization vibration data at high temperatures (∼1000 °F). The primary objectives included the following:

- Verify the Thermal Vibrational Test System (TVTS) methodology and analysis for combined load environmental testing.
- Evaluate the performance of commercially available high-temperature (HT) accelerometers under a radiant quartz lamp environment.
- Test ability of various configurations of signal conditioning hardware to mitigate effects of HT piezoelectric resistance loss [1] in accelerometers.

Test Fixture

The test fixture consisted of a stainless-steel two-story heatsink top plate designed to hold high-temperature accelerometers on the top surface under a radiant quartz lamp heat input. The two-story design provided a thermal brake between the high-temperature test environment and low-temperature shaker hardware while maintaining adequate stiffness to transfer dynamic loads in the frequency range of interest. This two-story plate was bolted to a magnesium vibration fixture that attached to an Unholtz Dickie (Unholtz Dickie Corporation, Wallingford, Connecticut) T100 500-lbf shaker. A thermal and electrical barrier of flame retardant (FR5) G-11 sheet was placed between the test fixture and the magnesium fixture, as shown in Fig. 1**(a)**. A summary of the test fixture components, shown in Fig. 1**(a),** is listed in **Table 1**. The dimensions of the test fixture is shown in **Fig. 1**(**b**). The total testable area on top of the heatsink was approximately 6- by 6-in.

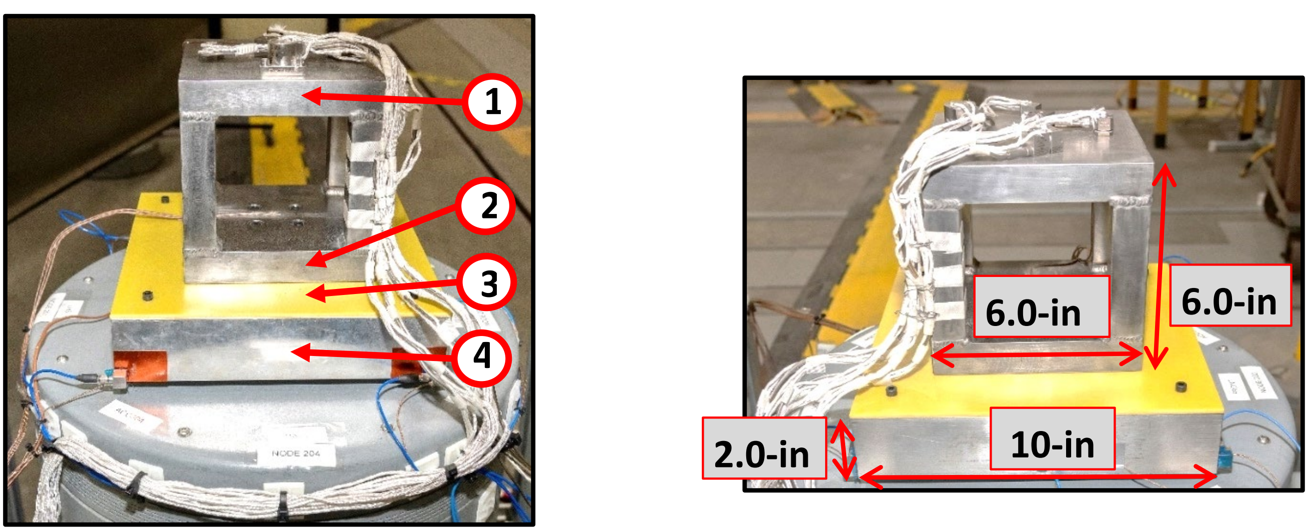

(a) (b)

Fig. 1 **(a)** TVTS pathfinder, test fixture heatsink and magnesium fixture mounted on top of Unholtz Dickie T100 shaker, and **(b)** TVTS test fixture heatsink and fixture dimensions

Table 1 TVTS test fixture and magnesium fixture material details

Number	Component	Material	Weight [lbs]
1	Test fixture heatsink top plate and supporting bars	Stainless Steel 304	25.0
2	Test fixture heatsink bottom plate	Steel A36	
3	Thermal electrical insulating barrier	Garolite G-11/FR5	0.9
4	Magnesium fixture	Magnesium AZ31B	12.5
Total weight			38.4

Material Selection

A material design space considered constraints such as material melting temperatures, thermal heatsink performance, shaker operational temperature limit and dynamic transmissibility. The target test temperature requirement was 1000 °F to be applied on high-temperature accelerometers. A heatsink was designed to dissipate thermal energy so that the maximum temperature of the fixture was less than the shaker operational temperature limit of 100 °F. Simultaneously, the stiffness-to-weight ratio had to be evaluated to make maximum use of the fixture mass [2]. Resonance is determined primarily by stiffness and mass (weight), a relationship characterized by the ratio of the modulus of elasticity, *E*, and density, ρ, (**Eq.** (1))**:**

$$\frac{E}{\rho} \tag{1}$$

This ratio is approximately 10^8 for metals that are suited for vibration fixtures such as steel, aluminum, and magnesium. The natural frequency of the test fixture had to rest outside of the test frequency range. The natural frequency was evaluated initially by considering a uniform cantilevered rod with the cantilevered rod vibrating in the vertical direction (**Eq.** (2)), with the moment of inertia of the rod cross-section (**Eq.** (3)):

$$f_n = \frac{1.76}{\pi}\left(\frac{EIg}{WL^3}\right)^{1/2} \tag{2}$$

$$I = \frac{bh^3}{12} \tag{3}$$

$$\frac{f}{f_n} \leq 0.8 \tag{4}$$

Where *g* is acceleration of gravity, *W* is the weight, *L* is the length of the rod, *b* is the base, *h* is the height, *f* is the forcing frequency, and f_n is the natural frequency. The fixture was kept as small as possible to reduce mass and keep effective spring rates high [7]. Dynamic transmissibility was addressed by keeping an acceptable forcing frequency to natural frequency ratio (**Eq.** (4)) of less than 0.8 since resonant amplification occurs when the frequency ratio is very near one [8]. The material selection in the material design space was confirmed by the analytical modeling found in **section 5**.

Test Setup

The thermal vibration test was conducted in the FLL High Bay area during the spring of 2025 [9], [10]. A primary frame was placed above the shaker to hold a single 36-kW quartz lamp heater with perimeter-surrounding insulating alumina fences, as shown in **Fig. 2**. A secondary inner, shorter frame was placed horizontally above the shaker to hold additional horizontal alumina sheets, providing a 6- by 6-sq in aperture for the heatsink test fixture. The alumina fences served as an insulating boundary around the quartz lamp heater to trap thermal radiation. The quartz lamp heater provided the thermal load into the thermal control region (the area within the alumina fences) via radiation, as shown in **Fig. 3**. The quartz lamp operated at 480 V with air cooling. Insulated blankets were placed around the test setup to reduce convective currents and to protect hardware and personnel. The candidate high-temperature accelerometers were mechanically fastened to the top surface of the heatsink test fixture and were exposed to radiant heat. The primary and secondary frames were bolted into the lab floor. A fan was placed over a lift table and aligned to the height of the heatsink to cool down the test fixture more rapidly after test completion. A shaker amplifier and cooling blower were placed in the vicinity for shaker cooling during operation.

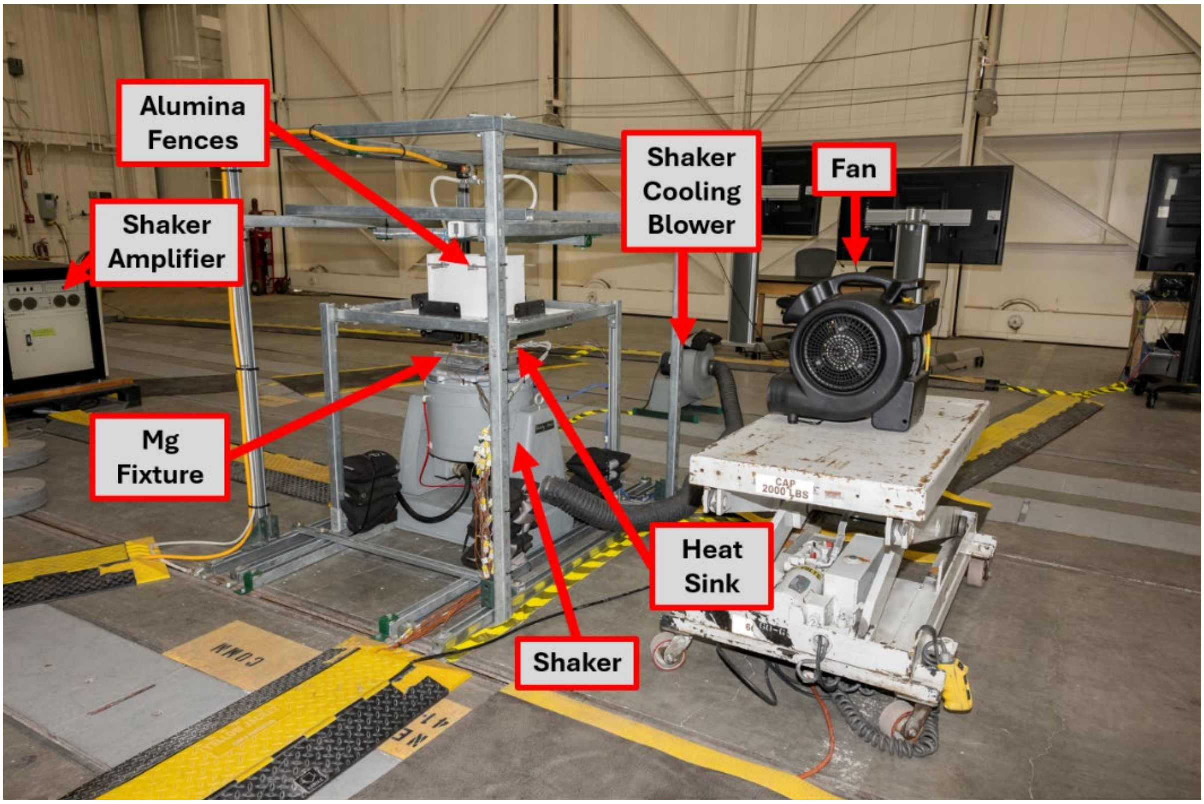

Fig. 2 TVTS test fixture heatsink and fixture mounted over shaker under quartz lamp heater

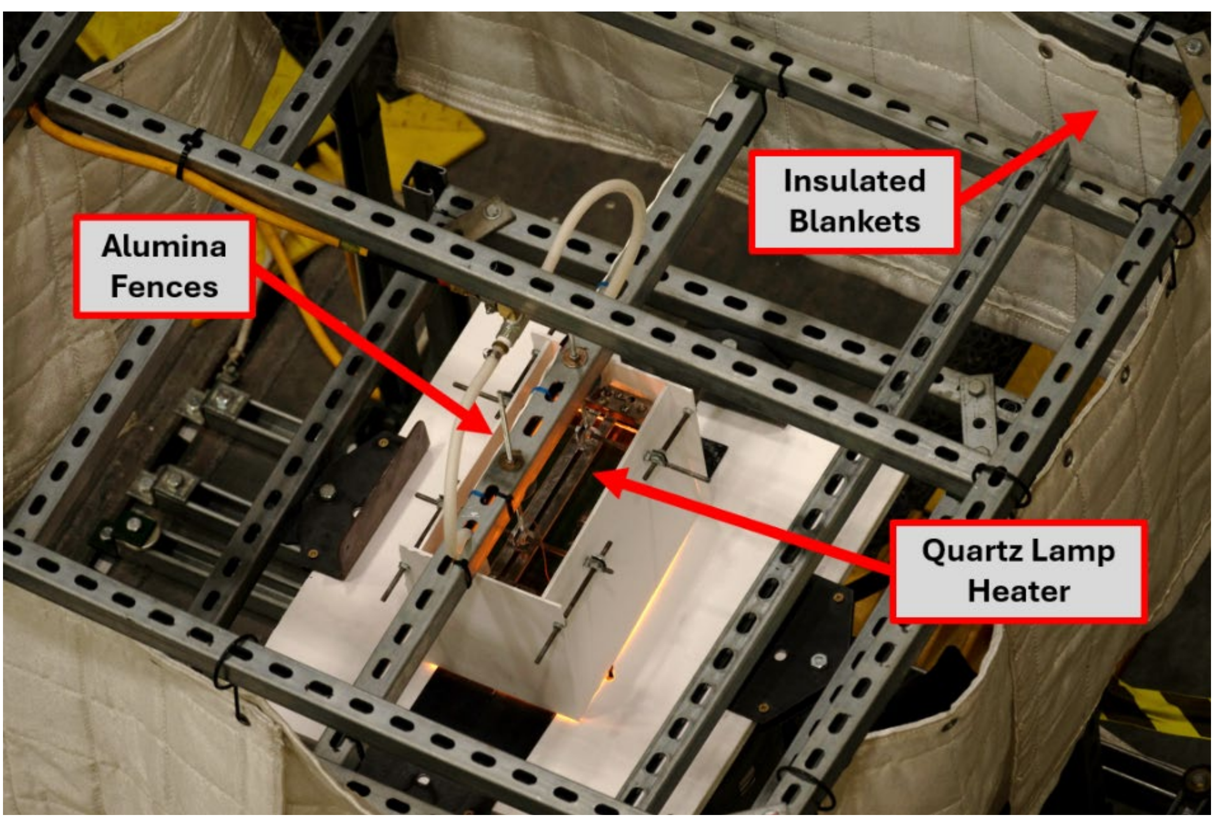

Fig. 3 TVTS test fixture heatsink and fixture mounted over shaker under quartz lamp heater

Pre-Test Design Analysis

Analytical modeling and analyses were completed to ensure that the heating system could achieve desired ramp rates and that the low-temperature hardware would not overheat. In addition, a modal analysis was conducted to ensure test fixture natural frequencies were outside of the testing frequency range to avoid resonance. For the pathfinder test series, a stepped quasi-constant temperature profile was developed. This profile included eight-minute thermal soaks at 200 °F, 500 °F, 700 °F, 900 °F, and 1000 °F. These soak durations were designed such that an incrementally stepped-vibration profile sequence (up to 3 grms) could be executed at quasi-constant temperature. An initial thermal screening was planned to assess the test setup heat transfer performance prior to the stepped quasi-constant temperature profile. This thermal screening subjected the accelerometer sensors and the test fixture to a maximum heat soak at 1000 °F for eight minutes plus an additional ramp-up time.

Thermal Soak Analysis

A conservative thermal heat soak at 1000 °F for the entire duration of the thermal screening profile of 38 minutes was modeled using COMSOL® Multiphysics simulation software. A simple and conservative transient thermal model was built to ensure that all low-temperature test hardware remained within temperature limits during the planned holds at high temperatures. A 1000 °F temperature boundary condition was applied to the top surface of the heatsink fixture, and room temperature convection was applied to the exposed lower surfaces of the fixture. The analytical results for a thermal soak at 1000 °F for 38 minutes are shown in **Fig. 4**. Most of the heat was found to dissipate via the temperature rise of the steel.

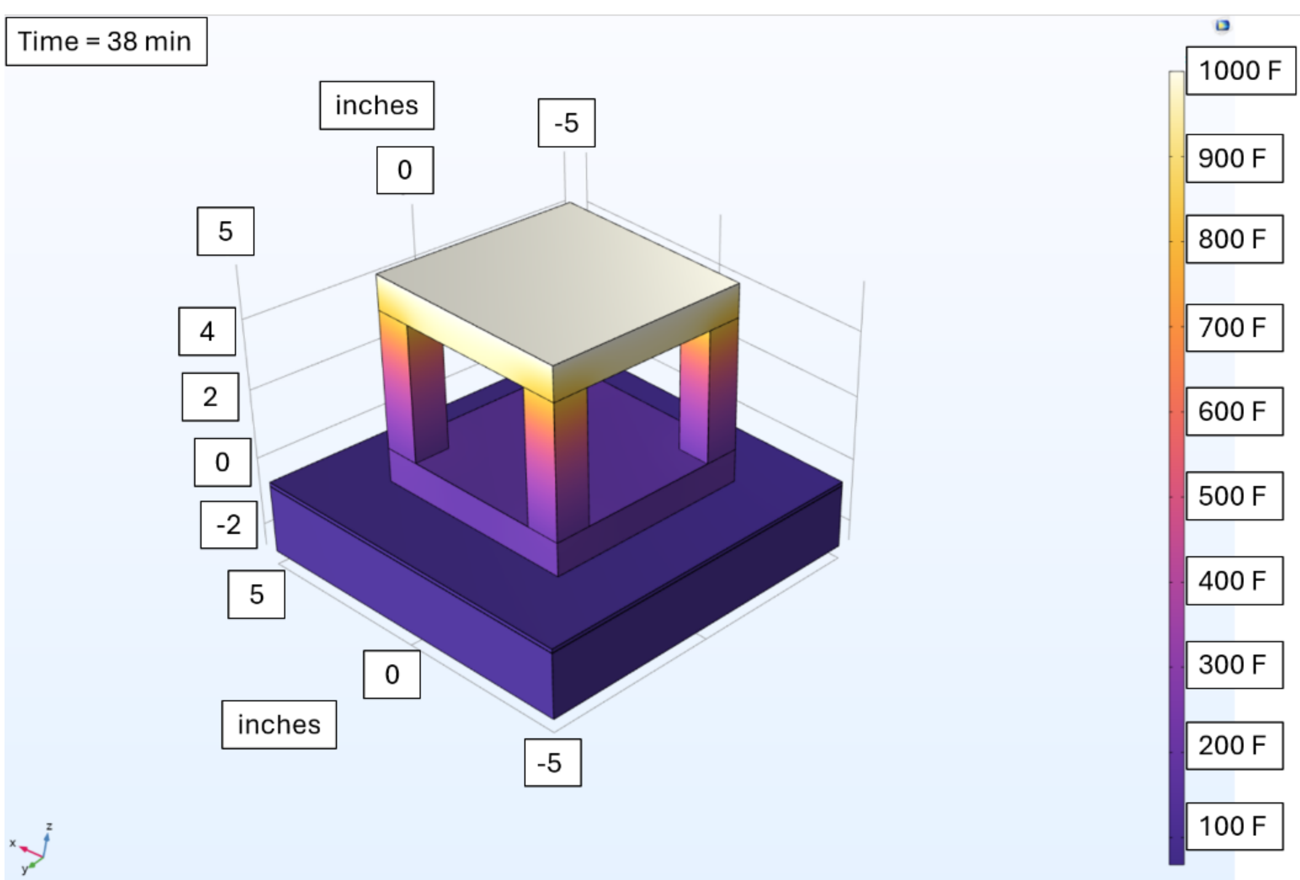

Fig. 4 Heat transfer from a 1000 °F heat soak for 38 minutes

Thermal Ramp Rate Analysis

A benchmark heater ramp rate of 80 °F/min was identified for transient temperature simulations. To ensure that the planned heater configuration could achieve this ramp rate, a second transient COMSOL® Multiphysics analysis was performed. The radiation from the quartz lamp was modeled at maximum power, as shown in **Fig. 5**. The ramp rate at maximum power was found to be 229 °F/min. Note that during testing, a ramp rate of 20 °F/min was used to achieve desired thermal gradients within the accelerometer bodies and thermal system controllability.

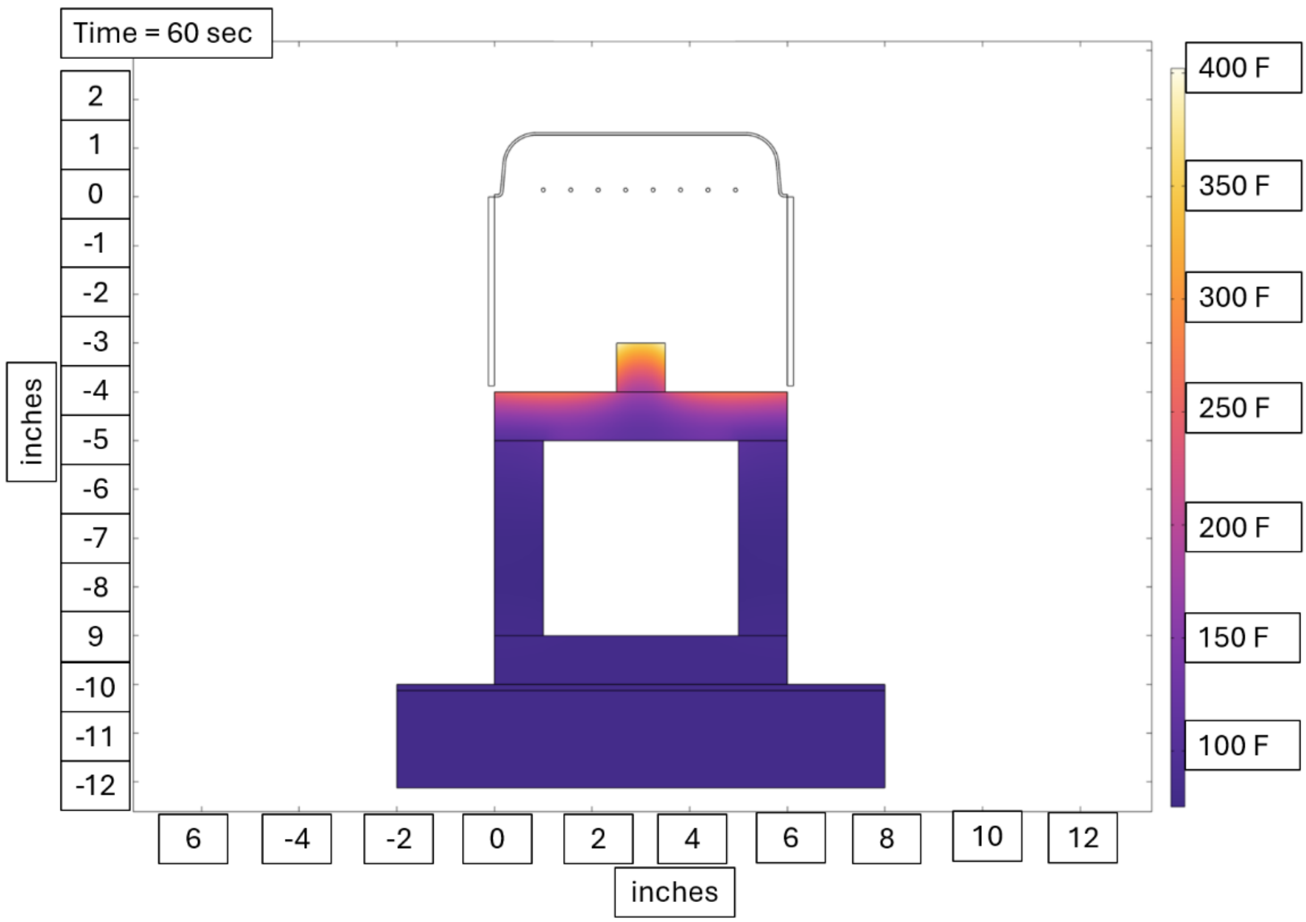

Fig. 5 Quartz lamp bulbs radiating at maximum power over the control accelerometer

Modal Analysis

For the pathfinder test series, the natural frequencies of the test fixture had to rest outside of the test frequency range to avoid amplification of dynamic loads and damage to test equipment [6]. The heatsink test fixture was set to be exposed to vertical excitation using random vibration test specifications at a maximum of 3 grms over a 5 – 300 Hz frequency range. An analytical model was built in Creo Parametric (now "Creo") 3D modeling software prior to testing to find the mode shapes, as shown in **Fig. 6**. A modal analysis at room temperature was executed with six degrees of freedom, and fixed boundary conditions at the shaker armature bolt circle pattern attachments. The material properties for each component were evaluated at 1000 °F to ensure the test fixture could transfer the dynamic loads at high temperature with **Eq.** (1).

Vibration Test Equipment

The vibration equipment utilized in this test includes high-temperature single-ended and differential charge accelerometers (rated to at least 1000 °F) from PCB Piezotronics (Depew, New York) and Dytran (Dytran by HBK, Chatsworth, California,

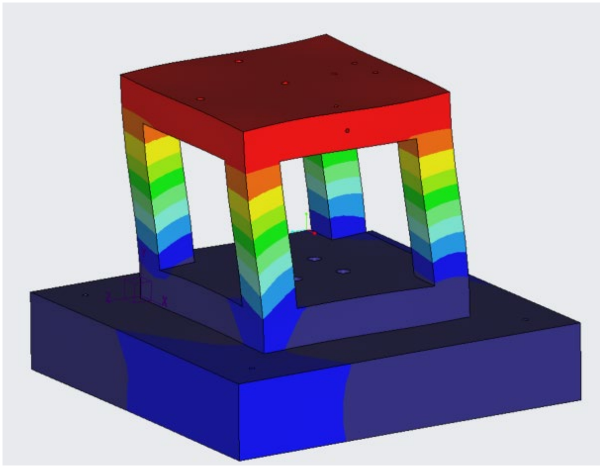

(a) [720 Hz] Heatsink in-plane sway with symmetric magnesium fixture in-plane sway

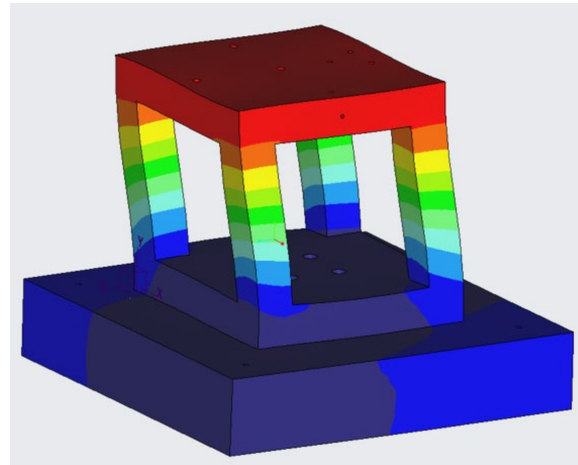

(b) [721 Hz] Heatsink out-of-plane sway with symmetric magnesium fixture out-of-plane sway

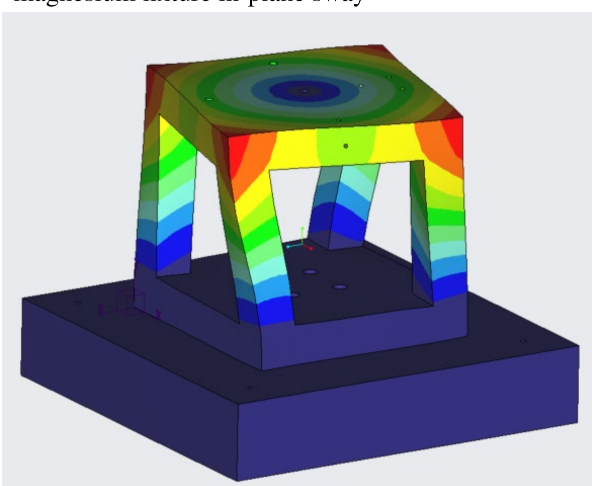

(c) [1,145] Heatsink table twist

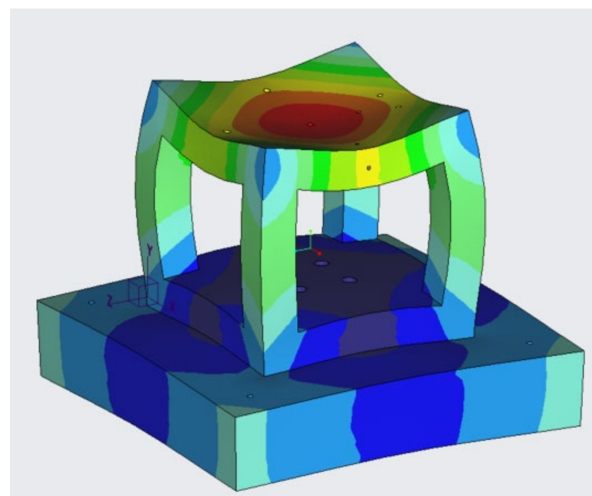

(d) [2,382] Heatsink 1st bending with symmetric magnesium fixture slight 1st bending

Fig. 6 Test fixture heatsink and magnesium fixture first four analytical mode shapes: **(a)** 720 Hz, **(b)** 721 Hz, **(c)** 1,145 Hz and **(d)** 2,382 Hz

formerly Dytran Instruments, Inc.), uniaxial standard Integrated Circuit Piezoelectric (ICP) accelerometers from PCB® and Dytran, Unholtz Dickie T100 shaker (500 lbf). Software consisted of the Sandia National Laboratory "Rattlesnake" vibration controller [11], and Hottinger Brüel & Kjær (HBK) (Darmstadt, Germany) BK Connect® vibration test software. Data acquisition and signal conditioning hardware consisted of an HBK LAN-XI 4-channel input plus 2-channel output 3160 module, a LAN-XI 6-channel 3050 module, one LAN-XI 5-slot mainframe, LAN-XI front panels 6-channel Charge UA-2120, 6-channel Differential (UA-2119, UA-2100, UA-2113), PCB®, and Dytran in-line charge amplifiers and the Precision Filters, Inc. (PFI) (Ithaca, New York) 28000 signal conditioning system.

Thermal Test Equipment

The thermal test equipment includes a 36-kW radiant-quartz lamp gold-coated heater, K-type thermocouples, a Pacific Instruments (PI) (Concord, California) 6000 data acquisition system, an Interactive Analysis and Display System (IADS) display software, the Power Control Cabinet (PCC) power system, the Thermal Controller System (TCS), and a fan.

Accelerometer Layout

High-temperature single-ended and differential charge uniaxial accelerometers were evaluated within the thermal control region. Uniaxial standard ICP accelerometers were used for vibration control and monitoring in areas where temperatures were under 250 °F. The HT accelerometers were located at the top plate of the heatsink test fixture (within the thermal control region surrounded by alumina fences). The majority of the ICP accelerometers were placed at the edges of the magnesium fixture to monitor plate-bending frequencies. The control ICP accelerometer was located directly underneath the magnesium fixture and on top of the shaker armature. This control accelerometer was used to drive the shaker armature vibration with the Sandia National Lab "Rattlesnake" vibration controller. The remaining accelerometer time histories were gathered with the HBK BK Connect® software. **Table 2** shows the accelerometer numbering scheme, number of locations, and number of channels for this test. A total number of 10 accelerometers were used with a total number of 10 channels. Accelerometer locations are shown in **Fig. 7**.

Table 2 Accelerometer Summary

Node series	Description	Accelerometer type	No. of locations	No. of channels
100	Control accelerometer	ICP	1	1
200	Top plate	HT single-ended and differential charge	5	5
300	magnesium fixture	ICP	4	4
Total accelerometers			**10**	**10**

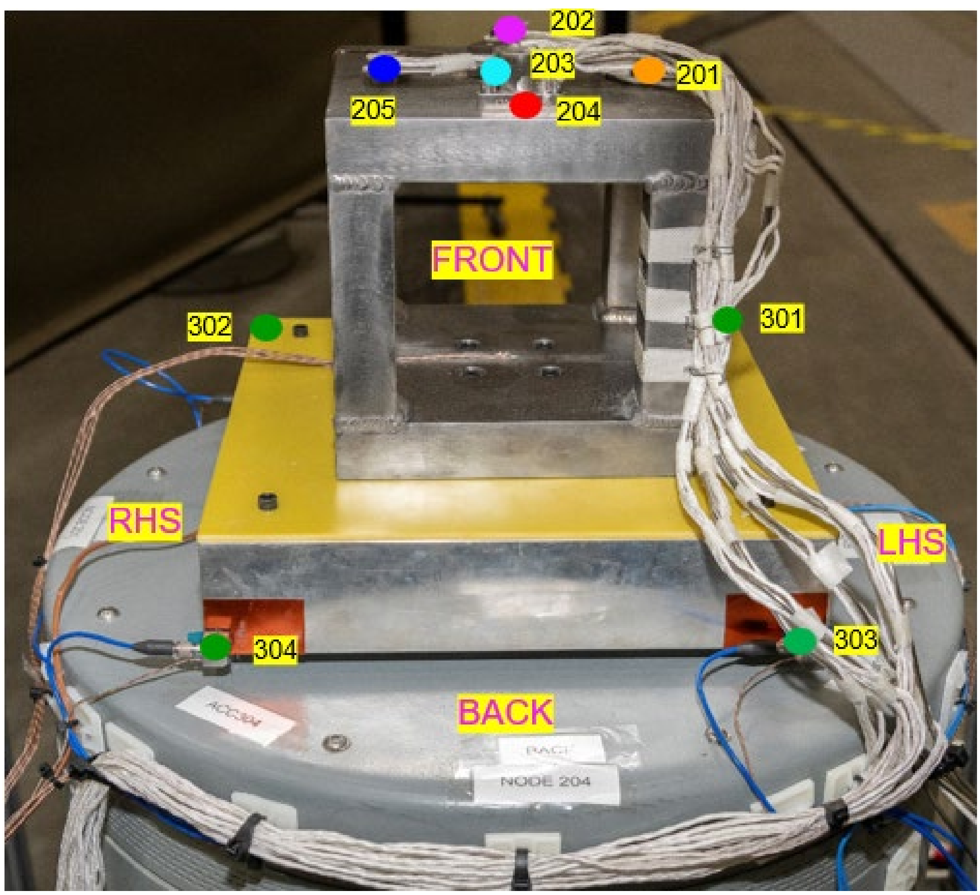

Fig. 7 Accelerometer locations

Thermocouple Layout

Each HT accelerometer was instrumented on the sensor housing with two thermocouples (TCs), with one on the top surface and the other on a side near the accelerometer base. A total of 25 thermocouples were used for this test, as shown in **Table 3.** The test fixture heatsink and the fixture were instrumented with Type-K thermocouples with high-temperature Nextel^{TM} (Newtex Industries, Victor, New York) heat-resistant braided rope. These thermocouples were installed with strain relief and formed via spot welding. Two thermocouples were used to monitor the magnesium fixture temperatures, as shown in **Fig. 8(a)**. A total of six thermocouples were placed at target heat transfer locations and are shown in red (**Fig. 8(b)**). **Fig. 9** shows an additional thermocouple that was installed on the quartz lamp heater to monitor quartz lamp reflector temperature as well as another thermocouple on the shaker.

Table 3 Thermocouple summary

Thermocouple channel name	Location description
ACC201_TOP	Accelerometer 201, top surface
ACC202_TOP	Accelerometer 202, top surface
ACC203_TOP	Accelerometer 203, top surface
ACC204_TOP	Accelerometer 204, top surface
ACC205_TOP	Accelerometer 205, top surface
ACC201_BOT	Accelerometer 201, bottom surface
ACC202_BOT	Accelerometer 202, bottom surface
ACC203_BOT	Accelerometer 203, bottom surface
ACC204_BOT	Accelerometer 204, bottom surface
ACC205_BOT	Accelerometer 205, bottom surface
TAHT1	Test fixture top-surface thermocouple, center, top
TAHT2	Test fixture top-surface thermocouple, center, bottom
TAHT3	Test fixture bar top-edge thermocouple
TAHT4	Test fixture bottom-edge thermocouple
TAHT5	Test fixture bottom-surface thermocouple, center
TAHT6	Test fixture surface thermocouple, region of interest
MGHT1	Cavity of magnesium fixture thermocouple
MGHT2	Magnesium fixture edge thermocouple
SHAKHT	Shaker thermocouple
ACC301_TOP	Accelerometer 301 left-hand-side front thermocouple, top
ACC302_TOP	Accelerometer 302 right-hand-side front thermocouple, top
ACC303_TOP	Accelerometer 303 right-hand-side back thermocouple, top
ACC304_TOP	Accelerometer 304 left-hand-side back thermocouple, top
ACC100_TOP	Control accelerometer top-surface thermocouple
QLAMP	Quartz lamp reflector temperature thermocouple
Total thermocouples	**25**

Test Configurations

The test described in this paper evaluated various accelerometers with various signal conditioning hardware to mitigate charge accelerometer signal noise due to impedance drop at elevated temperatures [1]. The five high-temperature accelerometers were conditioned in separate tests with three different signal conditioning configurations:

- **Configuration A:** Hottinger Brüel & Kjær (HBK) prototype front panels.
- **Configuration B:** PCB and Dytran in-line charge amplifiers.
- **Configuration C:** Precision Filter, Inc. (PFI) signal conditioning filter.

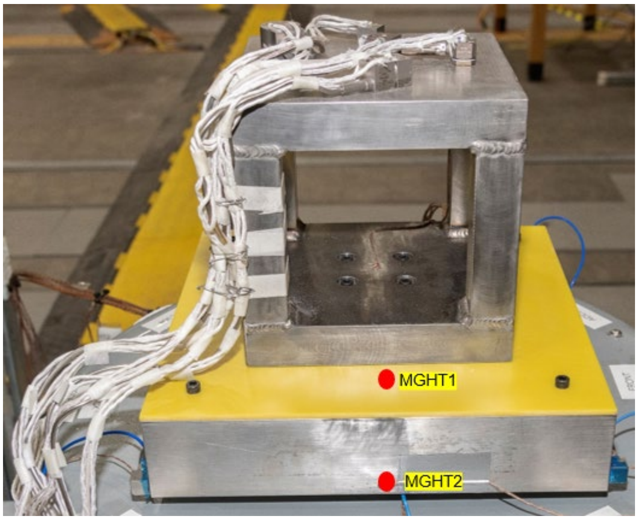

(a)

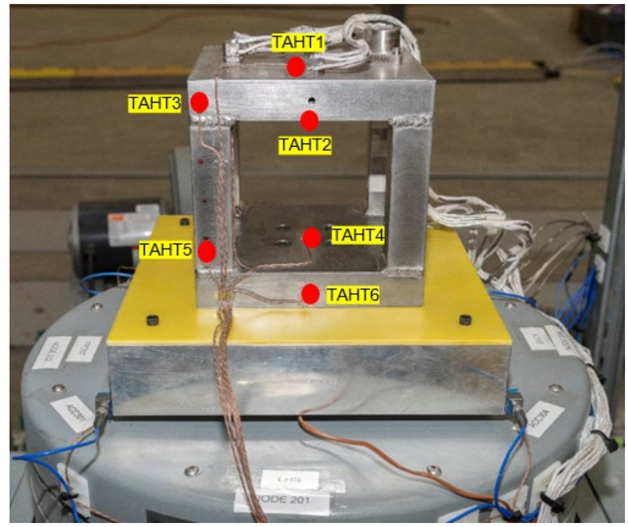

(b)

Fig. 8 **(a)** Thermocouples installed on magnesium fixture and **(b)** Heatsink fixture

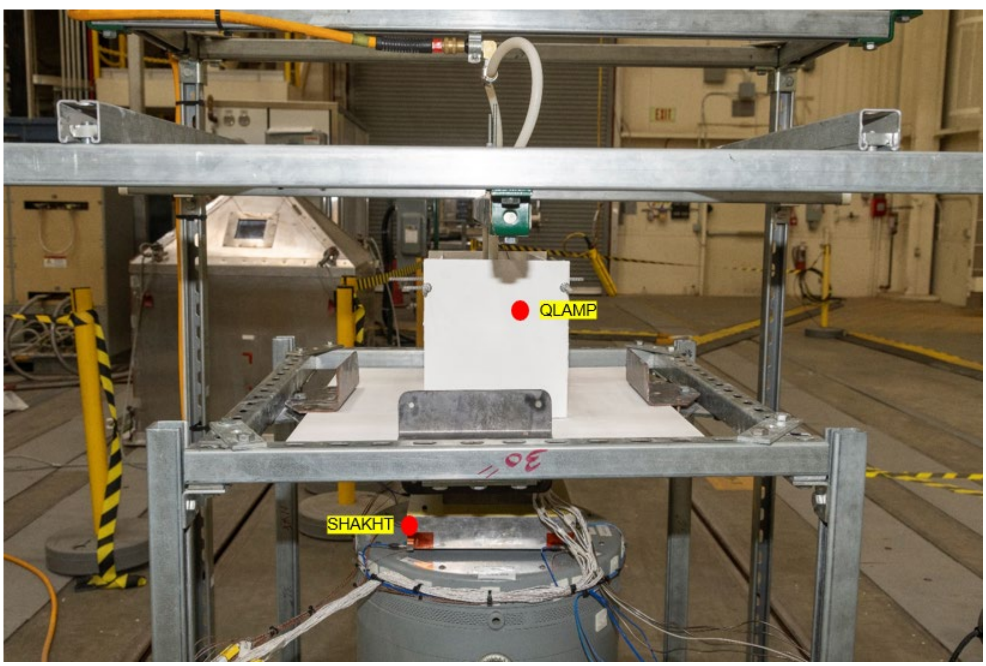

Fig. 9 Thermocouple locations on shaker and quartz lamp

The first test run cases were room-temperature vibration-only test cases with vibe profiles up to 3 grms for all three test configurations. A thermal load-only screening was executed to evaluate the survival of the sensors with a continuous ramp from room temperature to 1000 °F at 20 °F/min. Then, the combined thermal and vibration test cases (A3, B3, and C3) were executed for all test configurations with a vibration profile up to 3 grms and a thermal profile with temperature holds at 200 °F, 500 °F, 700 °F, 900 °F, and 1000 °F. Results for these three test cases will be discussed in the next section. **Table 4** shows the total number of tests runs for the test series. The separate vibration and thermal test runs helped identification and troubleshooting of any challenges before attempting the combined load test cases. The vibration-only test cases were executed to make sure the shaker had no operating issues and that the random vibration specification was being outputted correctly. The thermal screening test case was utilized to ensure that safety of test temperatures was within bounds as well as to refine the thermal controller gain and time constant for closed-loop control. The temperatures and random vibration outputs were monitored real time with IADS during testing on multiple thermal and vibration displays.

Table 4 Test configuration matrix for TVTS shakeout test

Test case	Config.	Hardware	Test case no.	Vibe profile [grms]	Thermal profile	Max temperature [°F]	Duration [min]	Number of runs
Random vibration	A	HBK front panels	A1	0.6, 1.5 & 3	-	68 - 74	10	1
	B	In-line charge amplifiers	B1	0.6, 1.5 & 3	-	68 - 74	10	1
	C	PFI signal conditioner	C1	0.6, 1.5 & 3	-	68 - 74	10	1
Thermal load	A	HBK front panels	A2	-	Screening	1000	51	1
	B	In-line charge amplifiers	B2	-	Screening	1000	51	1
	C	PFI signal conditioner	C2	-	Screening	1000	51	1
Combined thermal & vibrational loads	A	HBK front panels	A3	0.6, 1.5 & 3	Step profile	1000	75	1
	B	In-line charge amplifiers	B3	0.6, 1.5 & 3	Step profile	1000	75	1
	C	PFI signal conditioner	C3	0.6, 1.5 & 3	Step profile	1000	75	1
Total number of runs								**9**

Results

The random vibration test cases (A1 to C1) and then the thermal load test cases (A2 to C2) were executed independently in a buildup approach to verify the controllers and data acquisition systems were working properly. The thermocouples and accelerometers were examined independently to troubleshoot any issues before confirming the thermal- and vibration-profile load outputs against the controller inputs. After successfully completing the random vibration test cases (A1 to C1) and the thermal load test cases (A2 to C2), the combined load test cases (A3 to C3) were executed by simultaneously running both controllers and data acquisition systems.

The time histories and thermal profiles of the five different high-temperature accelerometers (**Table 2** and **Fig. 7**) for test cases A3 to C3 are shown in **Figs. 10** to **12**. The HT single-ended charge accelerometers are nodes 201, 202, and 203, whereas the HT differential charge accelerometers are nodes 204 and 205. The thermal profiles are plotted over the time histories for the top- and bottom-surface thermocouples on the high-temperature accelerometers in nodes 201 to 205. The accelerometer mass and location under the footprint of the quartz lamp influences the actual thermal profile applied to each individual accelerometer. The HT accelerometer at node 204 had the greatest mass and size and therefore showed the greatest temperature difference between the top and bottom surface, as shown in the different test cases (**Figs. 10(d)** to **12(d)**). The maximum temperature difference recorded between the top and bottom surface of the accelerometer at node 204 was 121 °F when the accelerometer top surface went above a 1000 °F (test case C3), as shown in **Fig. 12(d)**.

The control accelerometer shows the vibration output of the shaker and is plotted against the high-temperature accelerometer for nodes 201 to 205, as shown in **Figs. 10** to **12**. The differential charge accelerometers at nodes 204 and 205 show an increase in noise in test case A3 when compared to the single-ended charge accelerometers in nodes 201 to 203, as shown in **Figs. 10** and **12** (except for node 202)**.** The differential charge accelerometers nodes 204 and 205, however, show lower noise levels in test case B3, as shown in **Fig. 11**.

The accelerometer at node 203 shows more acceleration in all configurations when compared to the control accelerometer due to a believed calibration coefficient issue, as shown in **Figs. 10** to **12**. The same result for accelerometer 203 was observed in a different stationary heating oven test setup(results not included in this paper).

For test case C3, the differential charge accelerometers at nodes 204 and 205 show an increase in noise at higher temperatures, as shown in **Figs. 12(d)** and **(e)**. The single-ended charge accelerometer at node 202 shows unreasonably high levels of noise for test case C3 which is believed to be due to a ground isolation issue.

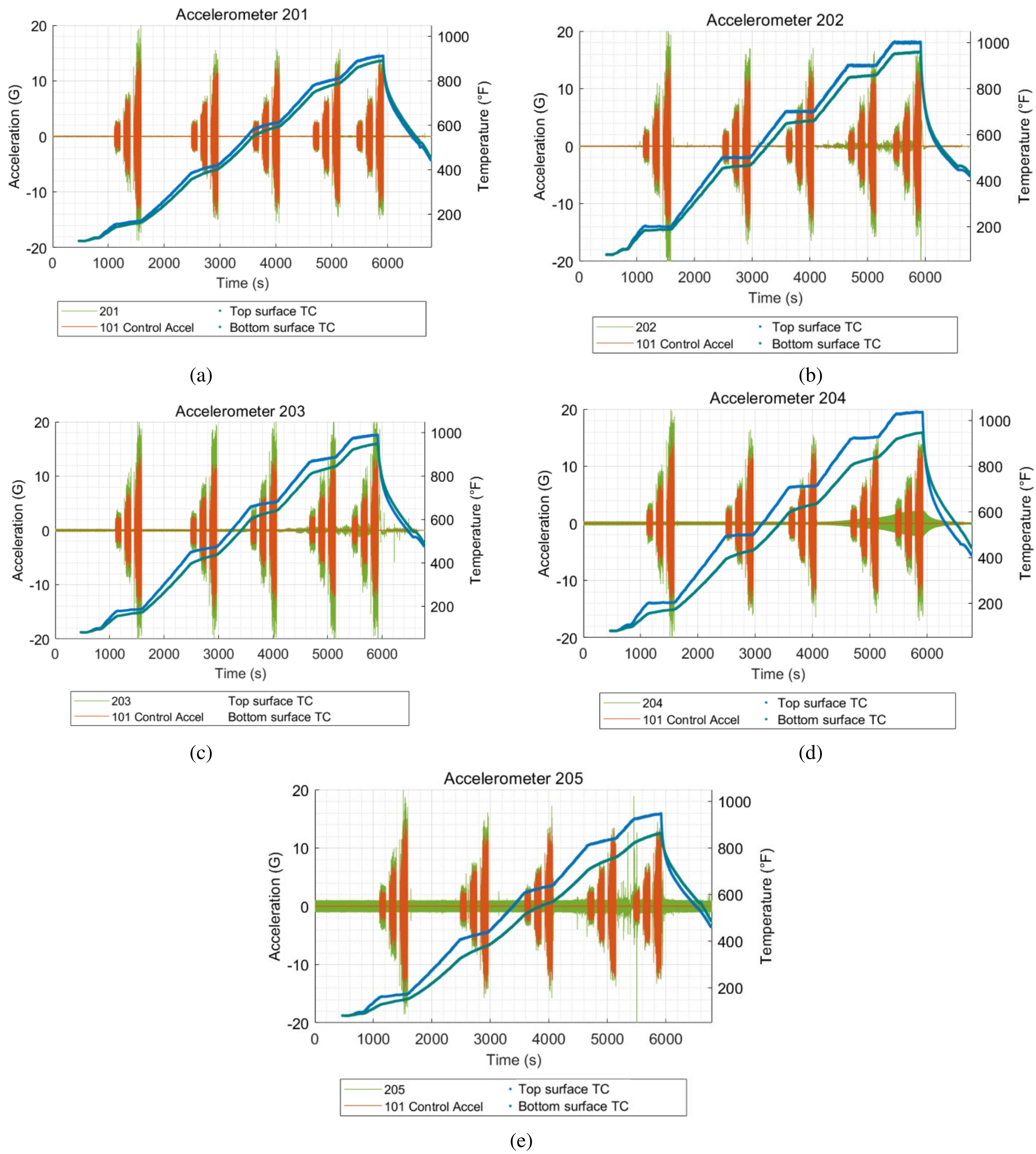

Fig. 10 Time histories for test case A3 (combined thermal and vibration loads with HBK front panels) for HT accelerometers at nodes **(a)** 201 **(b)** 202 **(c)** 203 **(d)** 204 and **(e)** 205

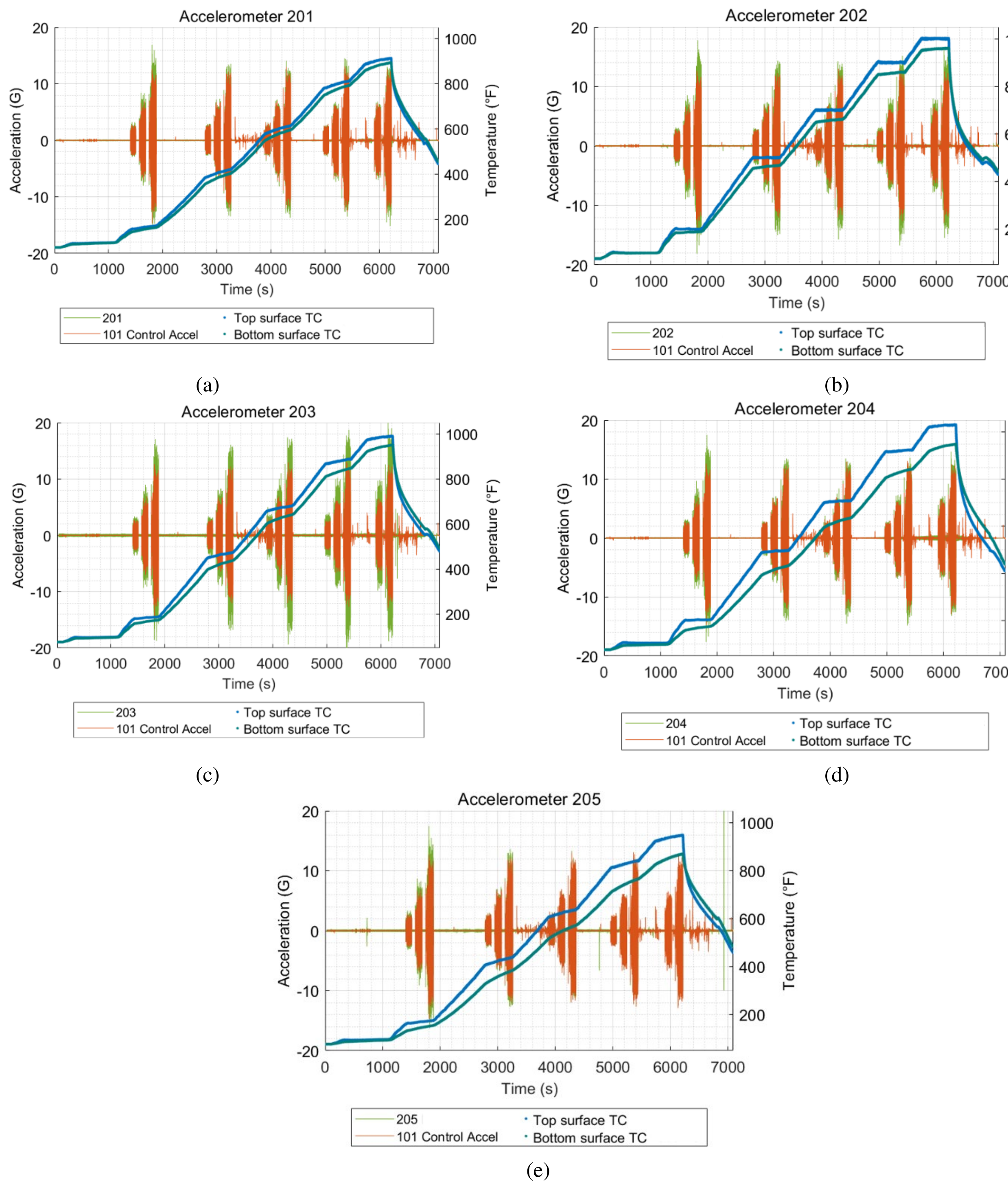

Fig. 11 Time histories for test case B3 (combined thermal and vibration loads with in-line charge amplifiers) for HT accelerometers at nodes **(a)** 201 **(b)** 202 **(c)** 203 **(d)** 204 and **(e)** 205

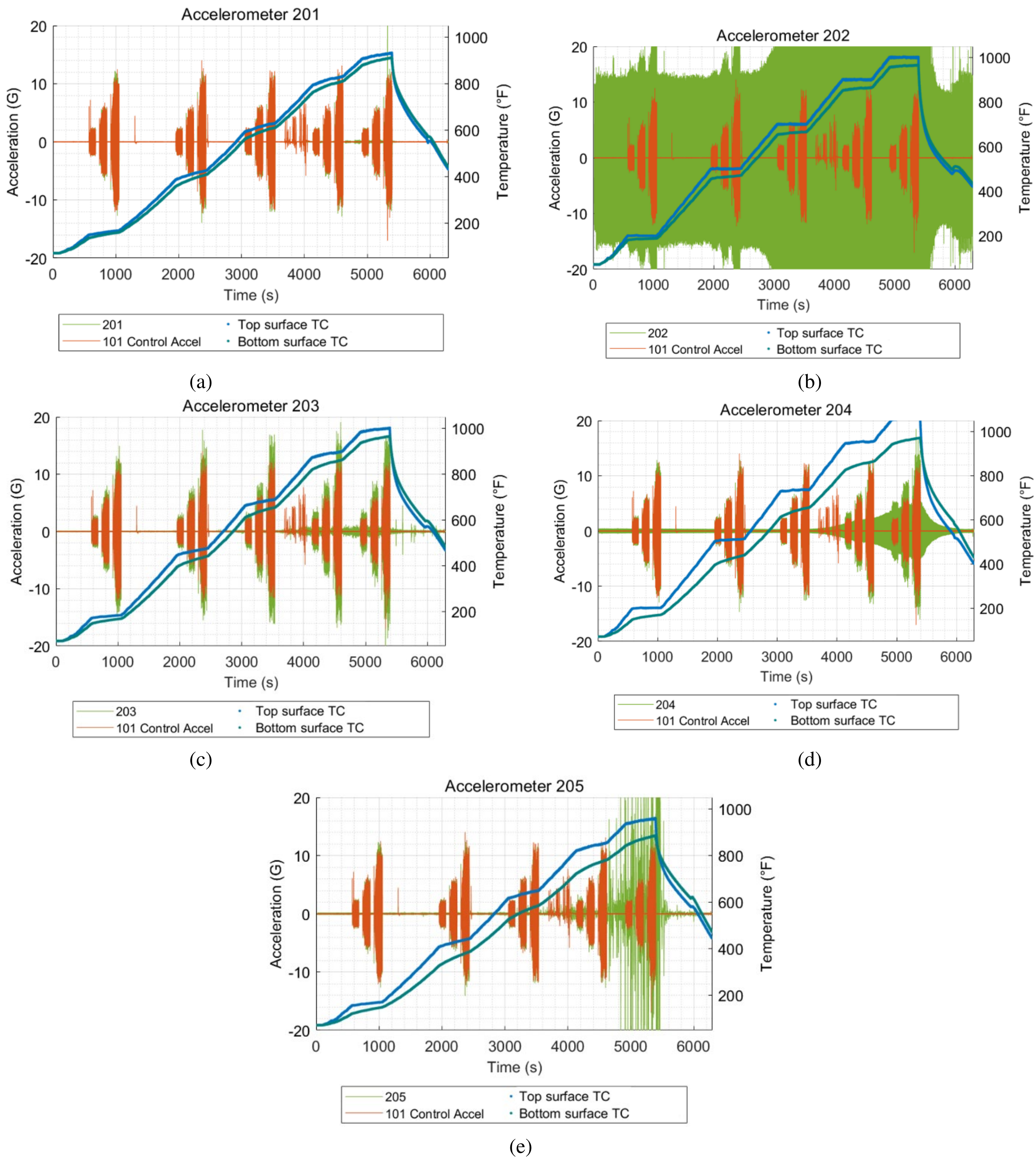

Fig. 12 Time histories for test case C3 (combined thermal and vibration loads with PFI signal conditioner) for HT accelerometers at nodes **(a)** 201 **(b)** 202 **(c)** 203 **(d)** 204 and **(e)** 205

The power spectral density (PSD) for the 3 grms vibe profile is plotted for each nominal thermal soak temperature for single-ended charge and differential charge accelerometers in nodes 201 to 205 (**Figs.** 13 to 17). Electrical noise valleys are seen at 60 and 180 Hz for all nodes and test configurations from either an unknown heater or setup isolation issue. Test cases A3 and B3 PSD curves showed a peak near 250 Hz due to the presence of loose bolts, as shown in **Fig.** 13(**b**). The bolts were observed to loosen after every thermal shake due to a coefficient of thermal expansion mismatch between the bolts and the test fixture. A requirement to torque the bolts was enforced prior to running test case C3. This behavior was also observed for all accelerometers from nodes 201 to 205 for test cases A3 and B3, as shown in **(a)** and **(b)** for **Figs.** 13 to 17.

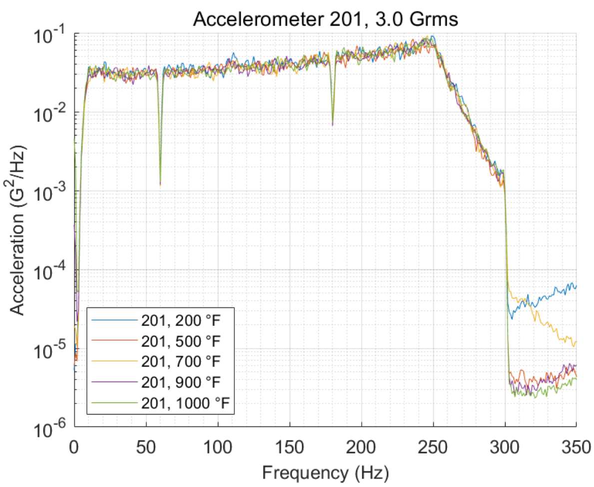

(a) Test case A3 (combined thermal and vibration loads with HBK front panels)

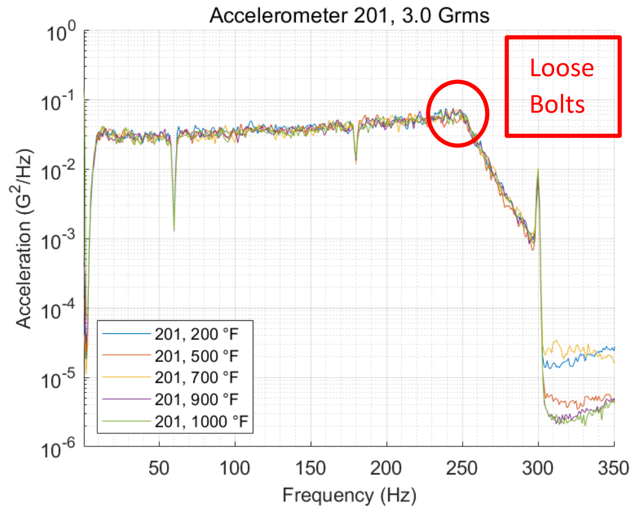

(b) Test case B3 (combined thermal and vibration loads with in-line charge amplifiers)

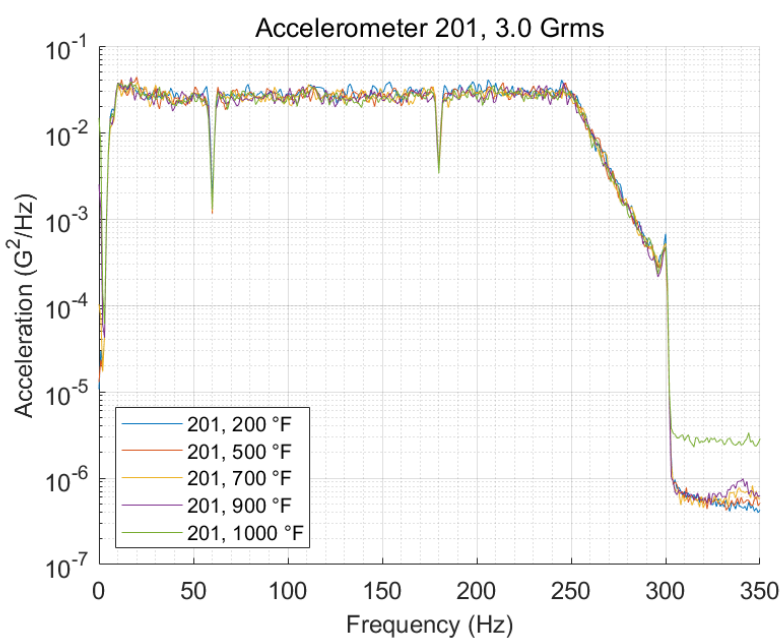

(c) Test case C3 (combined thermal and vibration loads with PFI signal conditioner)

Fig. 13 Output PSD for HT accelerometer at node 201 at different temperatures for **(a)** Test case A3 (combined thermal and vibration loads with HBK front panels), **(b)** test case B3 (combined thermal and vibration loads with in-line charge amplifiers) and **(c)** test case C3 (combined thermal and vibration loads with PFI signal conditioner)

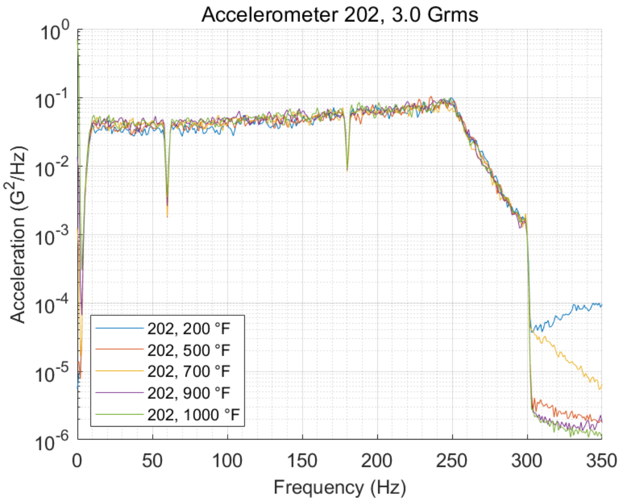

(a) Test case A3 (combined thermal and vibration loads with HBK front panels)

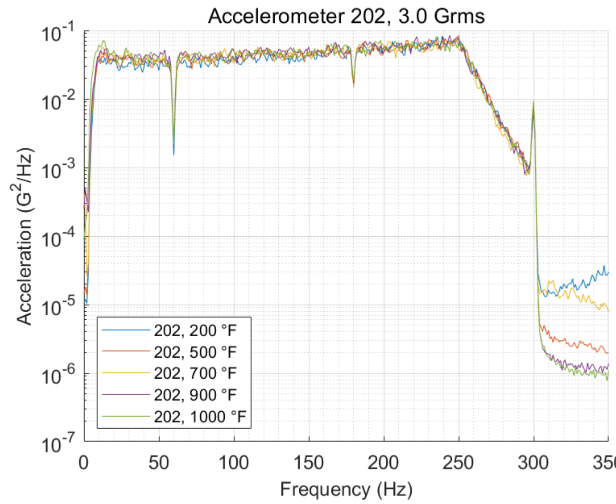

(b) Test case B3 (combined thermal and vibration loads with in-line charge amplifiers)

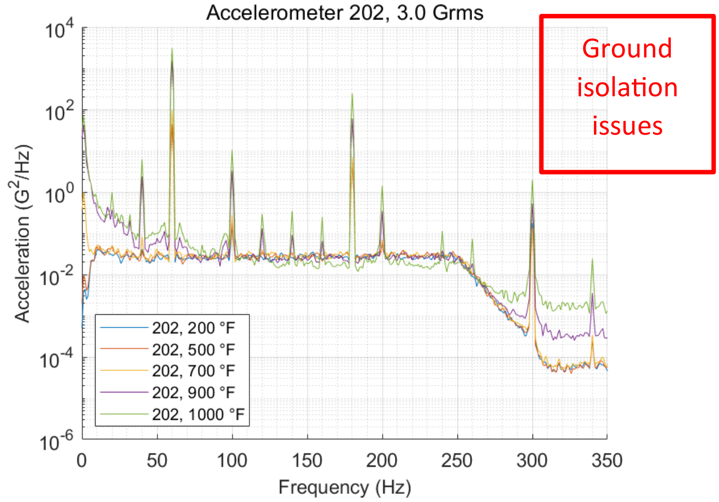

(c) Test case C3 (combined thermal and vibration loads with PFI signal conditioner)

Fig. 14 Output PSD for HT accelerometer at node 202 at different temperatures for **(a)** test case A3 (combined thermal and vibration loads with HBK front panels) **(b)** test case B3 (combined thermal and vibration loads with in-line charge amplifiers) and **(c)** test case C3 (combined thermal and vibration loads with PFI signal conditioner)

The high-temperature accelerometer in node 202 is believed to have an incidental ground isolation issue for test case C3, as shown in **Figs. 14(c)** and **12(b)**. Electrical noise and ground loops are seen to alter the vibration data and introduce unreasonable unwanted noise peaks in the output PSD frequency range. The differential accelerometer in node 204 shows significant noise level peaks at the electrical noise frequencies 60 and 180 Hz for test cases B3 and C3, as shown in **Figs. 16(b)** and **(c)**.

The change of temperature did not affect the 3 grms output PSD drastically within the specification frequency range for accelerometers in nodes 201 to 205, as shown in **Figs. 13** to **17**. The highest temperature recorded for the top plate of the two-story heatsink from TAHT1 was 880 °F, which was less than the 38-minute thermal soak analytical screening prediction of 1000 °F. The highest temperature recorded for TAHT6 (near the mounting boundary of the test fixture heatsink to the magnesium fixture) was 175 °F, which was nowhere near the 329 °F predicted by the 38-minute thermal soak analytical screening. The highest temperature recorded for SHAKHT was 85 °F. The heat transfer into the shaker did not exceed the

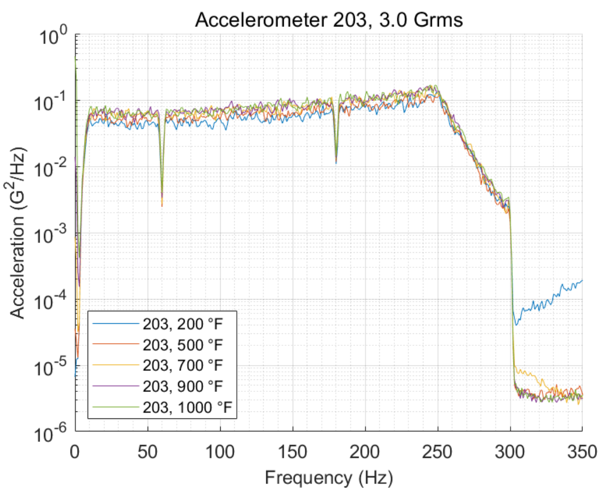

(a) Test case A3 (combined thermal and vibration loads with HBK front panels)

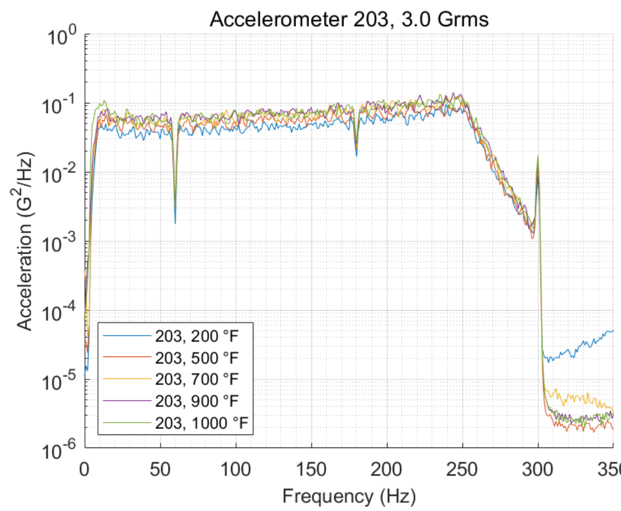

(b) Test case B3 (combined thermal and vibration loads with in-line charge amplifiers)

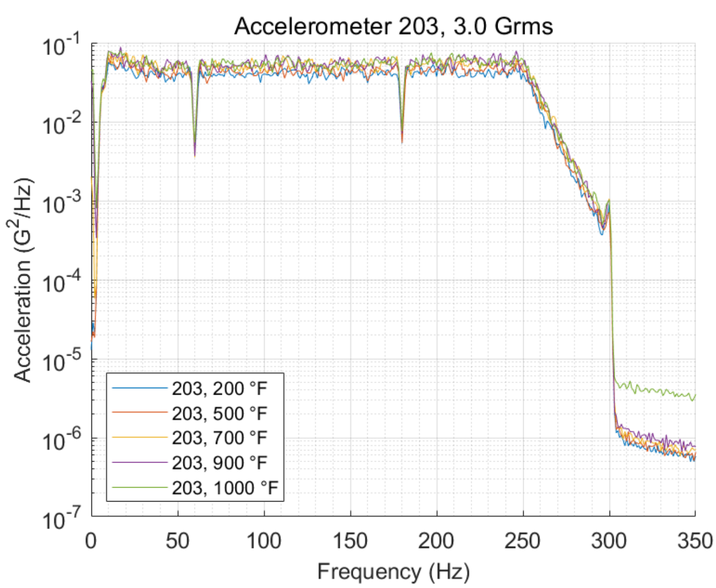

(c) Test case C3 (combined thermal and vibration loads with PFI signal conditioner)

Fig. 15 Output PSD for HT Accelerometer at node 203 at different temperatures for **(a)** test case A3 (combined thermal and vibration loads with HBK front panels) **(b)** test case B3 (combined thermal and vibration loads with in-line charge amplifiers) and **(c)** test case C3 (combined thermal and vibration loads with PFI signal conditioner)

low-operational shaker temperature limit of a 100 °F. No amplification of resonant frequencies was found within the testing range of 5 – 300 Hz.

Conclusions

The signal quality of the power spectral densities (PSDs) from each accelerometer with signal conditioning hardware combination was unique. The influence of the thermal and vibration environment was found to loosen test fixture bolts, and it is recommended to check torque periodically prior to testing. Electrical noise valleys were observed at 60 and 180 Hz for

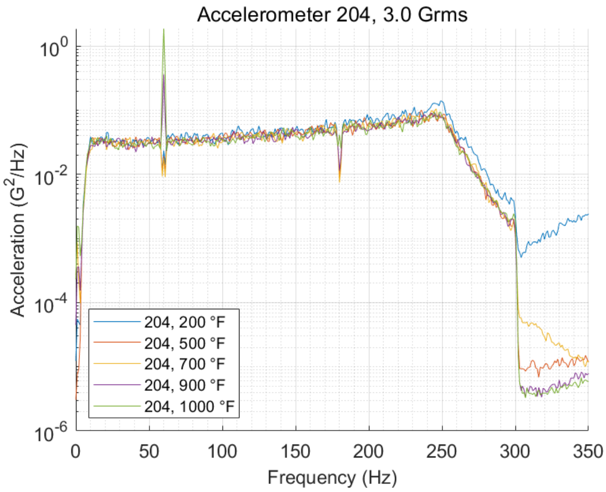

(a) Test case A3 (combined thermal and vibration loads with HBK front panels)

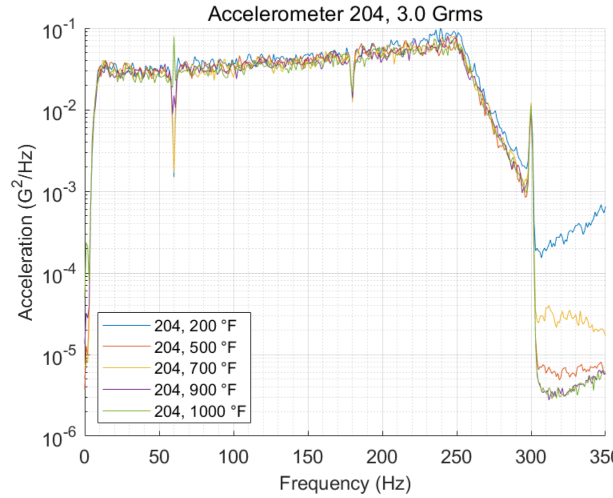

(b) Test case B3 (combined thermal and vibration loads with in-line charge amplifiers)

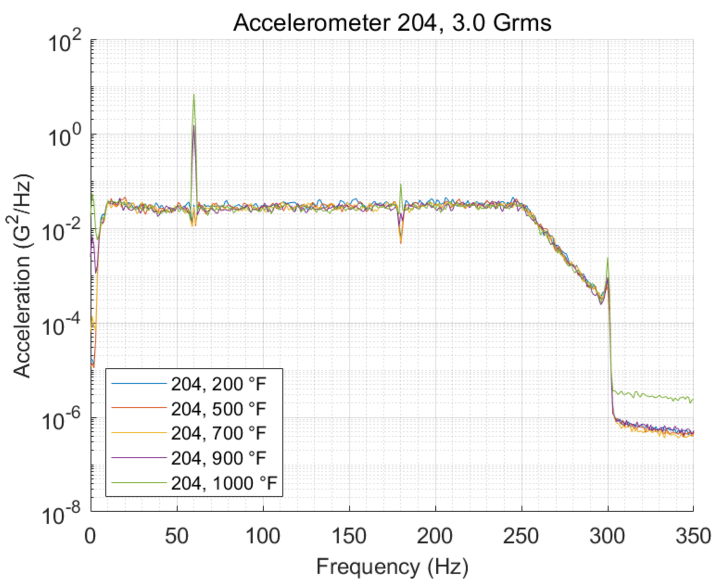

(c) Test case C3 (combined thermal and vibration loads with PFI signal conditioner)

Fig. 16 Output PSD for HT accelerometer at node 204, at different temperatures for **(a)** test case A3 (combined thermal and vibration loads with HBK front panels) **(b)** test case B3 (combined thermal and vibration loads with in-line charge amplifiers) and **(c)** test case C3 (combined thermal and vibration loads with PFI signal conditioner)

all nodes and test configurations. The change of temperature did not affect the 3 grms output PSD drastically within the specification frequency range for nodes 201 to 205. Further testing will confirm if this result is consistent for higher grms vibration profiles with different test fixture weights and thermal cooling properties. The accelerometer and thermal time histories along with the output PSDs show that the NASA Armstrong new testing capability can apply the random vibration test specification and the thermal load, simultaneously.

The single-ended and differential charge accelerometers performed similarly in the radiant quartz lamp environment used during this pathfinder test. The single-ended charge accelerometers in nodes 201 to 203 required commercially available 10-32 connector cables, whereas the differential accelerometers required unique cable connectors that were not as readily commercially available. The higher price of the differential accelerometers is a tradeoff to assess since they did not

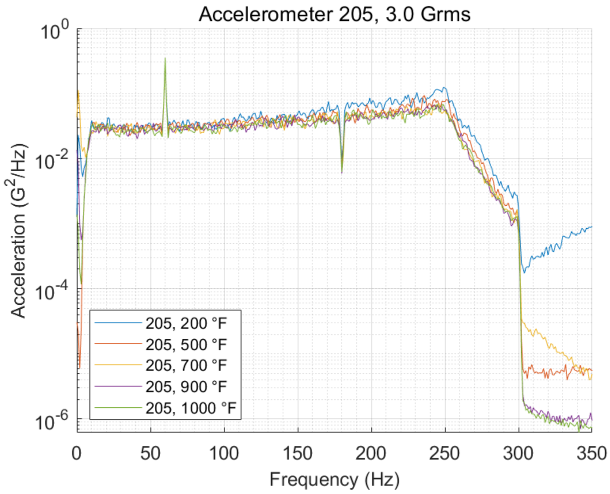

(a) Test case A3 (combined thermal and vibration loads with HBK front panels)

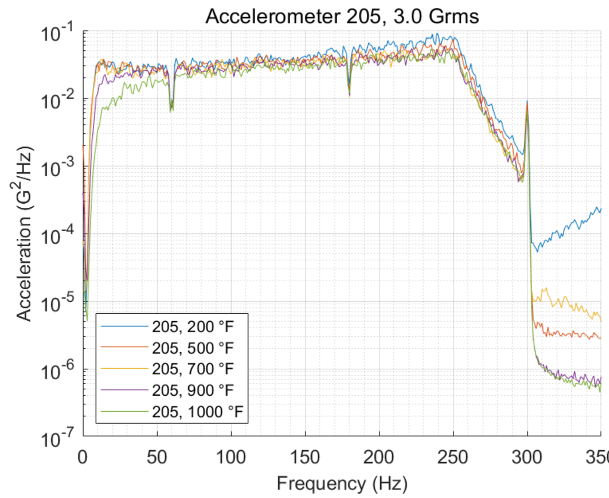

(b) Test case B3 (combined thermal and vibration loads with in-line charge amplifiers)

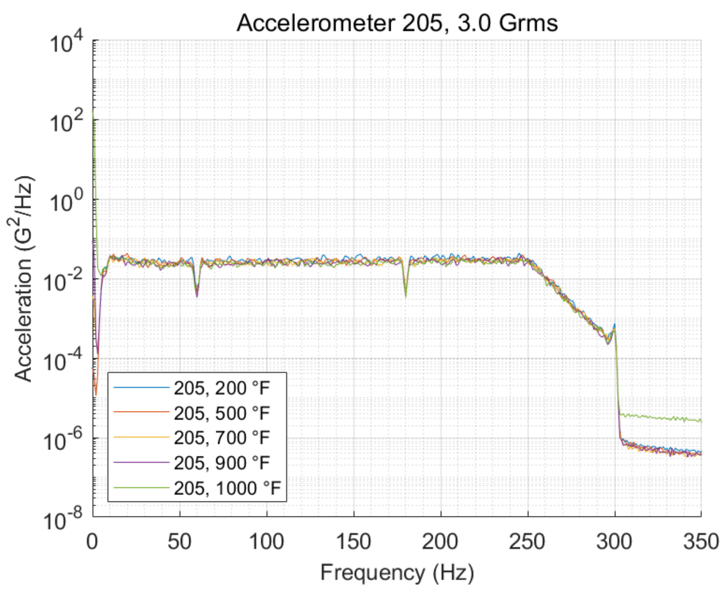

(c) Test case C3 (combined thermal and vibration loads with PFI signal conditioner)

Fig. 17 Output PSD for HT accelerometer at node 205, at different temperatures for **(a)** test case A3 (combined thermal and vibration loads with HBK front panels) , **(b)** test case B3 (combined thermal and vibration loads with in-line charge amplifiers) and **(c)** test case C3 (combined thermal and vibration loads with PFI signal conditioner)

improve the signal quality greatly for this application. Size, mass, price, and connector cable availability are influencing factors to consider when selecting a high-temperature accelerometer for combined load testing. For the single air-cooled lamp quartz lamp setup used in the FLL, differential charge accelerometers were not needed to mitigate test environment noise.

The pathfinder Thermal Vibrational Test System (TVTS) test results show additional combined thermal vibration tests could be developed by following the analysis methodology and setup described in this paper. The Flight Loads Laboratory (FLL) plans to mature TVTS to a larger-scale environmental qualification capability for new high-temperature sensors. Several opportunities to evolve TVTS for larger scale testing include active cooling arrangements to thermally isolate fixtures, larger shakers, and vacuum chamber integration.

Acknowledgments The authors thank the AFRC FLL and the AFRC Code 560 Aerostructures personnel who supported planning and operations to test in the lab. The authors also thank Kevin Westhora from Dytran, Mike Powell from FLW, Inc., Doug Lovelace and Melissa Hall from HBK, Nicholas Schultz, Bob Metz and Roger Kenyon from PCB, and Alan Szary from PFI for providing hardware knowledge, purchase assistance, loaners and support.

References

1. Mayo, Scott, "Considerations For Using Charge Amplifiers With High Temperature Piezoelectric Accelerometers," Technical Paper 339, Endevco.
2. Hudson, Larry, and Stephens, Craig, "X-37 C/SiC Ruddervator Subcomponent Test Program," 2009 Annual Meeting, NASA Dryden Flight Research Center, Edwards CA, September 29, 2009.
3. Kehoe, Michael W., and Deaton, Vivian, "Correlation of Analytical and Experimental Hot Structure Vibration Results," NASA Technical Memorandum 104269, 1993.
4. Kehoe, Michael W., and Snyder, Todd H., "Thermoelastic Vibration Test Techniques," NASA Technical Memorandum 101742, April 1991.
5. Snyder, Todd H., and Kehoe, Michael W., "Determination of the Effects of Heating on Modal Characteristics of an Aluminum Plate with Application to Hypersonic Vehicles," NASA Technical Memorandum 4274, 1991.
6. Spivey, Natalie, "High-Temperature Modal Survey of a Hot-Structure Control Surface," 27^{th} International Congress of the Aeronautical Sciences (ICAS), 2010, Nice, France.
7. Steinberg, Dave S., "Vibration Analysis for Electronic Equipment," 3rd Ed., John Wiley & Sons, 2000.
8. Irvine, Tom, "An Introduction to Shock and Vibration Response Spectra," Revision E, August 23, 2023.
9. De la Cruz, Jessica, "NASA Armstrong's New Thermal Vibration Test System (TVTS) Capability," Conference Presentation, Structures, Loads & Dynamics, Materials, and Mechanical Systems (SLAMMS) 2025, July 8, 2025, Merritt Island, FL. Available from J. De la Cruz, Armstrong Flight Research Center, Edwards, CA 93523.
10. De la Cruz, Jessica, "NASA Armstrong's Thermal Vibration Test System (TVTS)," Conference Presentation, Structures, Loads & Dynamics, Materials, and Mechanical Systems (SLAMMS) 2024, July 23, 2024, Las Cruces, NM 88012. Available from J. De la Cruz, Armstrong Flight Research Center, Edwards, CA 93523.
11. Rohe, Daniel P., Schultz, Ryan, and Hunter, Norman, "Rattlesnake User's Manual," Version 3, Sandia National Laboratories, Printed: Oct. 2024, SAND2024-14378, Albuquerque, NM and Livermore, CA. doi.org/10.2172/2480206